Dynamic Response Study of RCC T-Beam Skew Superstructure

Miss. Soumyashree Pani[1], Prof. Dr. Pravat Kumar Parhi[2]
Department of Civil Engineering
[1] M Tech Scholar, College of Engineering and Technology, Bhubaneswar, India
[2] Professor, College of Engineering and Technology, Bhubaneswar, India.

Abstract- *Skew bridges are the most important structures of the modern transportation system. For these structures, earthquakes are the most difficult natural hazard to be designed for, due to their occurrence without any warning, wide range in its frequency and its extreme consequences. Despite many new advancements in the field of seismology, it is yet very difficult to predict the location, magnitude and time of occurrence of a particular earthquake. Functional bridges after a major seismic event not only provide effective evacuation path for residents, but also ensure connection of the seismic affected areas for emergency response personnel to render prompt recovery and retrofitting efforts.*

In this research study, an attempt has been made to know the structural behaviour of the skew bridges under various loading like dead load, live load and seismic load. The effect of variation of skew angle was noted on parameters like maximum bending moment and shear force using grillage analogy in STAAD Pro V8i and the results were plotted

Keywords- Skew Bridge, Skew Angle, Grillage Analogy, Maximum Bending Moment, Shear Force

I. INTRODUCTION

Bridges are considered as lifelines of the society as they serve various functions, most importantly they serve as a path to cross any obstacle like river, valley or any steam, etc. without destructing the passage beneath it. Bridges can be broadly classified as skew bridges and non-skew bridges depending upon the type of crossing. Skew bridges are provided in highways and railways where non-perpendicular or oblique crossings are found from one bank to the other. Various studies have been carried out to study the structural behaviour of these bridges.

In the present study, an analysis was carried out to know the structural behaviour of skew bridges due to variation in skew angle. The grillage analysis was carried out using STAAD Pro software. The effect of change in skewness was observed on various parameters like the bending moment, shear force, etc..

II. LITERATURE REVIEW

A significant number of researches have been carried out to know the structural behaviour of bridges, especially skew bridges under various loads. Some of those researches which were highly significant for this study are discussed below: K. Nguyen and J.M. Goicolea (2018) attempted to purpose a simplified model to determine the dynamic response of simply supported skew bridge under moving loads. They observed that the degree of skewness of the bridge plays a vital role in determining the dynamic behaviour of the bridge in terms of vertical displacement. They concluded that with increase in skew angle, the vertical displacement decreases. However, the vertical acceleration is not significantly affected by the skewness of the bridge.

Ajay D. Shahu, P. D. Pachpor and S.V. Joshi (2016) focused on understanding the effect of skew angle on skew bridges. They concluded that with increase in skew angle, torsional moment increases which there by increase the equivalent shear and equivalent bending moment too.

Nagashekhar J P et al. (2016) studied the effect of skewness on the reinforced concrete girder bridges. They concluded that for dead load with increase in skew angle , the maximum bending moment decreases whereas for live load with increase in skew angle , the maximum bending moment increases. They also said that with increase in skew angle the torsional forces increases.

III. METHODOLOGY

In the present study an attempt has been made to study the behaviour of skew bridges due to variation in skew angle of the bridge. Numerical modelling was performed through grillage analogy method in STAAD Pro V8i software. Grillage analogy is a simple method used to analyse the bridge decks and give a clear visualisation of the forces and loads applied on the girders. It is a versatile method since it can easily handle the skewness of the bridge and other geometric complications.

IV. MODELLING

Numerical modelling was performed through grillage analogy method in STAAD Pro V8i software. A total of 5 models were created for the present study by varying the skew angle of the models. The skew angle was varied between 0o to 60o with an interval of 15o each. The basic data about the numerical models are described in table 4.1.

TABLE 4.1: PRELIMINARY DATA USED IN MODELLING

Span c/c of expansion joints	14.00 m
Span c/c of bearings	13.00 m
Depth of superstructure at formation level	1.350 m
Depth of longitudinal girder	1.125 m
Thickness of slab	0.225 m
Thickness of wearing coat	0.075 m
C/c of bearing and expansion joint	0.280 m
Total width of superstructure	16.00 m
Width of carriageway	11.00 m
Dimension of footpath on RHS	(1.5) m x (0.3) m
Dimension of footpath on LHS	(1.5) m x (0.3) m
Dimension of crash barrier on RHS	(0.5) m x (1.1) m
Dimension of crash barrier on LHS	(0.5) m x (1.1) m
Dimension of railing on RHS	(0.5) m x (1.1) m
Dimension of railing on LHS	(0.5) m x (1.1) m
Dimension of safety kerb on LHS	(0.0) m x (0.0) m
Dimension of safety kerb on RHS	(0.0) m x (0.0) m
C/C distance between girders	3.000 m
Cantilever projection of slab from c/c of outer girder	2.000 m
Total no. of longitudnal girders	5
Total no. of cross girders	3
Skew angle	$0^o/15^o/30^o/45^o/60^o$
Material property (a) Unit weight of concrete (b) Unit weight of wearing coat	 25 kN/m^3 22 kN/m^3

The details of each model is mentioned in table 4.2.

TABLE 4.2: DETAILS OF THE MODELS

Model 1	Model with 0^o skew angle
Model 2	Model with 15^o skew angle
Model 3	Model with 30^o skew angle
Model 4	Model with 45^o skew angle
Model 5	Model with 60^o skew angle

Various loads were applied on the bridge as per IRC 6:2016. The details of the applied loads are mentioned below:

A. Dead load:

The different parts of the bridge were subjected to different amount of load. The detailed descriptions of the dead load applied on the models were given in table 4.3.

TABLE 4.3: DETAILS OF DEAD LOAD APPLIED ON THE MODELS

Description	**Area (m^2)**	**Density (kN/m^3)**	**Load**	**Load Type**
<u>Superimposed Dead load(w/o surfacing)</u>				
Railing	0.55	25.00	13.75	UDL
Kerb	0.00	25.00	0.00	UDL
Crash Barrier	0.55	25.00	13.75	UDL
Footpath	0.45	25.00	11.25	UDL
<u>Superimposed Dead Load(only surfacing)</u>				
Wearing Coat		22.0	1.65	FLOOR
<u>Self weight of Outer Girder with deck slab</u>				
End Section	1.6	25.0	39.3	UDL
Tapered Section	1.5	25.0	39.3 to 33.6	LVL
Mid Section	1.3	25.0	33.6	UDL
<u>Self Weight of Inner Girder with deck slab</u>				
End Section	1.4	25.0	34.3	UDL
Tapered Section	1.3	25.0	34.3 to 29.5	LVL
Mid Section	1.2	25.0	29.5	UDL

Where,
LVL = Linearly varying load (in kN/m)
UDL= Uniformly distributed load(in kN/m)
FLOOR = Floor load (in kN/m2)

B. Live load:

For three lane carriageway structure, as per IRC 6-2016 (Table 6A) following live load combinations has been considered for the analysis of the numerical models.

i. Class 70 R (Wheeled) + Class A vehicles
ii. Class A+ Class A+ Class A vehicles

C. **Footpath live load**

According to clause 206.3 of IRC 6:2016 , for bridge with effective span of 13 m the footpath live load was calculated as per equation 1 mentioned below.

$$P = P' - \left(\frac{40L-300}{9}\right) \quad \text{............... (Equation 1)}$$

Where,

P = Intensity of footpath live load

P' = 500 or 400 kg/m2

L = Effective span of main girder (m)

W = Width of Footpath

The calculation of this load is tabulated in table 4.4 shown below

TABLE 4.4: CALCULATION OF FOOTPATH LIVELOAD

Description	Effective Span (m)	P' (kg/m^2)	Footway Width (m)	Intensity (kN/m^2)
Footpath Live Load (RHS)	13.00	500	1.50	4.76
Footway Live Load (LHS)	13.00	500	1.50	4.76

V. RESULTS AND DISCUSSIONS

A. Bending Moment

Bending moment can be of two types depending on their signs i.e. positive bending moment which is called as the sagging moment and negative bending moment which is called as the hogging moment. Bending moment depends on the load applied on the structure. Various loads like dead load, live load (vehicular load), seismic load was applied on the bridge superstructure. For each of these load, the bending moment developed on the longitudinal and cross girders of each model was noted and plotted and shown in figure 1 to 8.

A.1 Bending moment due to dead load and footpath live load

Figure 5.1 represented the maximum sagging bending moment due to dead load and footpath live load. The figure clearly indicated that the interior longitudinal girders had no sagging bending moment in all 5 models.. In case of longitudinal girders, the maximum value of sagging moment was observed for model 5 (model with 60o skew angle) for exterior longitudinal girder 2. Amongst the cross girders, the highest value was observed for interior mid cross girder in every model which decreased with increase in skew angle. In case of cross girders, the maximum value of sagging moment was observed for model 1 (model with 0o skew angle) for interior mid cross girder.

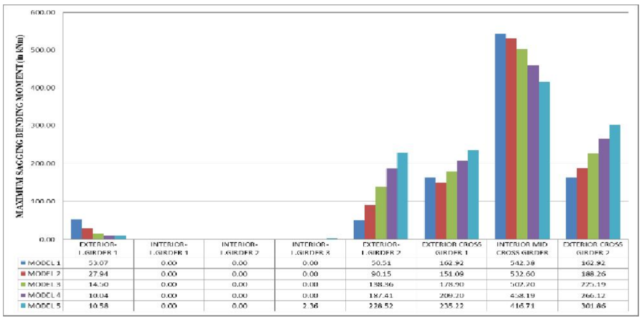

FIGURE 5.1: GRAPH SHOWING THE VARIATION OF MAXIMUM SAGGING MOMENT FOR VARIOUS MODELS UNDER DEAD LOAD AND FOOTPATH LIVE LOAD

Figure 5.2 represented the maximum hogging bending moment due to dead load and footpath live load. The figure clearly indicated that in all models except model 4 and 5(model with 45o and 60o skew angle respectively), exterior longitudinal girder 1(exterior l. girder 1) had lesser value of hogging moment as compared to exterior longitudinal girder 2(exterior l. girder 2) which increased with increase in skew angle. The hogging moment decreased with increase in skew angle in case of interior longitudinal girders. In case of longitudinal girders, the maximum value of hogging moment was observed for model 5 (model with 60o skew angle) for exterior longitudinal girder 1. Amongst the cross girders, no hogging moment value was observed for interior mid cross girder in any model. The hogging moment in the cross girders increased with increase in skew angle. In case of cross girders, the maximum value of hogging moment was observed for model 5 (model with 60o skew angle) for exterior cross girder 1.

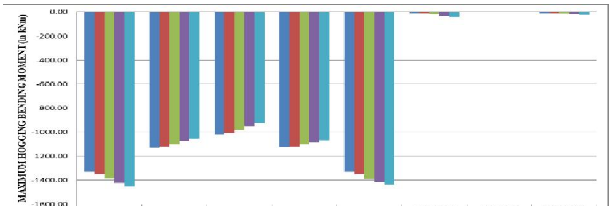

	EXTERIOR-L.GIRDER 1	INTERIOR-L.GIRDER 1	INTERIOR-L.GIRDER 2	INTERIOR-L.GIRDER 3	EXTERIOR-L.GIRDER 2	EXTERIOR CROSS GIRDER 1	INTERIOR MID CROSS GIRDER	EXTERIOR CROSS GIRDER 2
MODEL 1	-1334.75	-1129.10	-1020.87	-1121.78	-1335.17	-9.74	0.00	-9.74
MODEL 2	-1352.61	-1119.02	-1009.20	-1117.64	-1354.96	-11.07	0.00	-11.26
MODEL 3	-1388.93	-1098.39	-980.91	-1108.20	-1387.10	-19.32	0.00	-14.14
MODEL 4	-1420.73	-1075.02	-949.08	-1085.13	-1417.89	-29.98	0.00	-17.57
MODEL 5	1447.75	1055.54	923.76	1069.15	1440.14	39.93	0.00	20.83

FIGURE 5.2: GRAPH SHOWING THE VARIATION OF MAXIMUM HOGGING MOMENT FOR VARIOUS MODELS UNDER DEAD LOAD AND FOOTPATH LIVE LOAD

A.2 Bending moment due to live load

A.2.1 Live Load (Case 1 i.e., combination of Class 70 R (Wheeled) + Class A vehicles)

Figure 5.3 represented the maximum sagging bending moment under live load (case 1 which refers to the combination of Class 70 R (Wheeled) + Class A vehicles). The figure clearly indicated that in all models, the sagging moment increased with increase in skew angle in case of longitudinal girders. In case of longitudinal girders, the maximum value of sagging moment was observed for model 5 (model with 60^o skew angle) for interior longitudinal girder 3. Amongst the cross girders, the maximum sagging moment value was observed for interior mid cross girder in all models except model 5 (model with 60^o skew angle). The sagging moment in the cross girders increased with increase in skew angle. In case of cross girders, the maximum value of sagging moment was observed for model 5 (model with 60^o skew angle) for exterior cross girder 2.

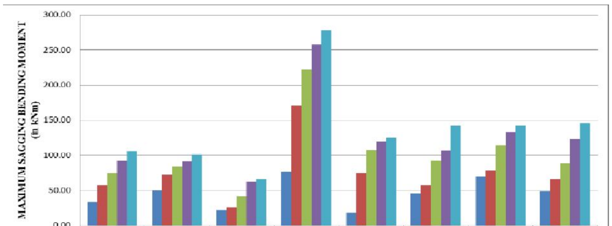

	EXTERIOR L.GIRDER 1	INTERIOR L.GIRDER 1	INTERIOR L.GIRDER 2	INTERIOR L.GIRDER 3	EXTERIOR L.GIRDER 2	EXTERIOR CROSS GIRDER 1	INTERIOR MID CROSS GIRDER	EXTERIOR CROSS GIRDER 2
MODEL 1	32.81	49.62	22.16	76.21	18.12	45.42	69.81	48.56
MODEL 2	56.98	71.69	25.54	169.87	74.67	57.28	77.73	66.11
MODEL 3	74.33	83.78	40.99	222.19	107.57	91.94	114.52	88.62
MODEL 4	92.23	91.30	62.50	258.03	119.73	107.19	132.90	123.49
MODEL 5	106.02	101.35	66.25	276.97	125.07	142.82	143.10	145.85

FIGURE 5.3: GRAPH SHOWING THE VARIATION OF MAXIMUM SAGGING MOMENT FOR VARIOUS MODELS UNDER LIVE LOAD (CASE 1 i.e., COMBINATION OF CLASS 70 R (WHEELED) + CLASS A VEHICLES)

Figure 5.4 represented the maximum hogging bending moment under live load (case 1 which refers to the combination of Class 70 R (Wheeled) + Class A vehicles). The figure clearly indicated that in all models exterior longitudinal girder 1(exterior l. girder 1) had lesser value of hogging moment as compared to exterior longitudinal girder 2(exterior l. girder 2) which decreased with increase in skew angle after 15^o.. However, interior longitudinal girder 2 had the maximum hogging moment amongst all interior longitudinal girders except for model 1 in which the maximum value was observed for interior longitudinal girder 3. The hogging moment decreased with increase in skew angle in case of interior longitudinal girders. In case of longitudinal girders, the maximum value of hogging moment was observed for model 2 (model with 15^o skew angle) for interior longitudinal girder 2 and minimum value was observed for model 1(model with 0^o skew angle) for exterior longitudinal girder 1(exterior l. girder 1). Amongst the cross girders, the maximum hogging moment value was observed for interior mid cross girder in all models. The hogging moment in the cross girders increased with increase in skew angle. In case of cross girders, the maximum value of hogging moment was observed for model 5 (model with 60^o skew angle) for interior mid cross girder.

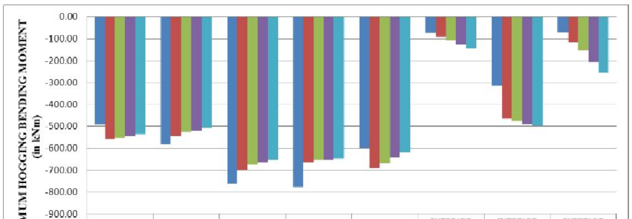

	EXTERIOR-L.GIRDER 1	INTERIOR-L.GIRDER 1	INTERIOR-L.GIRDER 2	INTERIOR-L.GIRDER 3	EXTERIOR-L.GIRDER 2	EXTERIOR CROSS GIRDER 1	INTERIOR MID CROSS GIRDER	EXTERIOR CROSS GIRDER 2
MODEL 1	-491.87	-583.03	-763.62	-777.03	-598.51	-75.14	-315.65	-72.08
MODEL 2	-557.52	-545.95	-698.96	-662.95	-692.03	-90.81	-465.73	-115.71
MODEL 3	-550.63	-524.84	-673.38	-652.18	-668.04	-106.64	-476.27	-152.67
MODEL 4	-544.18	-521.25	-661.98	-651.81	-642.65	-125.89	-489.78	-208.47
MODEL 5	-536.37	-509.28	-651.37	-646.61	-619.80	-144.91	-499.63	-256.66

FIGURE 5.4: GRAPH SHOWING THE VARIATION OF MAXIMUM HOGGING MOMENT FOR VARIOUS MODELS UNDER LIVE LOAD (CASE 1 i.e., COMBINATION OF CLASS 70 R (WHEELED) + CLASS A VEHICLES)

A.2.2 Live Load (Case 2 i.e., combination of Class A + Class A + Class A vehicles)

Figure 5.5 represented the maximum sagging bending moment under live load (case 2 which refers to the combination of class A + Class A + Class A vehicles) . The figure clearly indicated that the in all models, exterior longitudinal girder 2(exterior l. girder 2) had lesser value of sagging moment as compared to exterior longitudinal girder 1(exterior l. girder 1) which increased with increase in skew angle. In case of longitudinal girders, the maximum value of sagging moment was observed for model 5 (model with 60^o skew angle) for interior longitudinal girder 2. Amongst the cross girders, the maximum sagging moment value was observed for exterior cross girder 2 in all models except model 1 (model with 0^o skew angle) in which the maximum value was observed for interior mid cross girder. The sagging moment in the cross girder increased with increase in skew angle. In case of cross girders, the maximum value of sagging moment was observed for model 5 (model with 60^o skew angle) for exterior cross girder 2

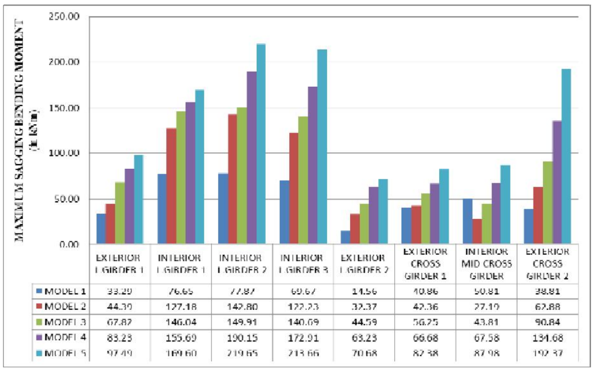

FIGURE 5.5: GRAPH SHOWING THE VARIATION OF MAXIMUM SAGGING MOMENT FOR VARIOUS MODELS UNDER LIVE LOAD (CASE 2 i.e., COMBINATION OF CLASS A + CLASS A + CLASS A VEHICLES)

Figure 5.6 represented the maximum hogging bending moment under live load (case 1 which refers to the combination of Class A + Class A + Class A vehicles). The figure clearly indicated that in all models exterior longitudinal girder 2(exterior l. girder 2) had lesser value of hogging moment as compared to exterior longitudinal girder 1(exterior l. girder 1) which decreased with increase in skew angle after 15^o. The interior longitudinal girder 2 had the maximum hogging moment amongst all interior longitudinal girders. The hogging moment decreased with increase in skew angle in case of interior longitudinal girders. In case of longitudinal girders, the maximum value of hogging moment was observed for model 1 (model with 0^o skew angle) for interior longitudinal girder 2. Amongst the cross girders, the maximum hogging moment value was observed for interior mid cross girder in all models. In case of cross girders, the maximum value of hogging moment was observed for model 2 (model with 15^o skew angle) for interior mid cross girder.

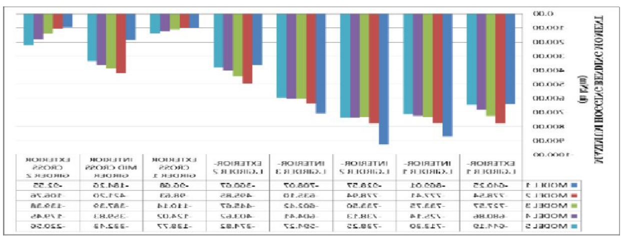

FIGURE 5.6: GRAPH SHOWING THE VARIATION OF MAXIMUM HOGGING MOMENT FOR VARIOUS MODELS UNDER LIVE LOAD (CASE 2 i.e., COMBINATION OF CLASS A + CLASS A + CLASS A VEHICLES)

A.3 Bending moment due to seismic load

Figure 5.7 represented the maximum sagging bending moment due to the seismic load in both x and z directions. The figure clearly indicated that for seismic load in both x and z direction (EQ X and EQ Z respectively), exterior longitudinal girder 1(exterior l. girder 1) had lesser value of sagging moment as compared to exterior longitudinal girder 2(exterior l. girder 2) which increased with increase in skew angle for all the models. Similarly, the interior longitudinal girder 3(interior l. girder 3) had highest value of sagging moment due to both EQ X and EQ Z for all the models. However, the value of sagging moment due to seismic load in x direction (EQ X) was greater than that of seismic load in z direction (EQ Z). In case of longitudinal girders, the maximum value of sagging moment was observed for model 5 (model with 60^o skew angle) for exterior longitudinal girder 2 under seismic load in x direction. Amongst the cross girders, the maximum sagging moment value was observed for exterior cross girder 2 in all models under the seismic load in z direction. The sagging moment in the cross girder increased with increase in skew angle. However, the value of sagging moment due to seismic load in z direction (EQ Z) was greater than that of seismic load in x direction (EQ X). In case of cross girders, the maximum value of sagging moment was observed for model 5 (model with 60^o skew angle) for exterior cross girder 2 under seismic load in z direction.

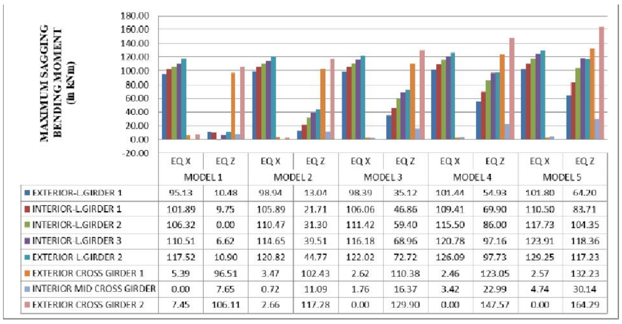

FIGURE 5.7: GRAPH SHOWING THE VARIATION OF MAXIMUM SAGGING MOMENT FOR VARIOUS MODELS UNDER SEISMIC LOAD IN BOTH X AND Z DIRECTION

Figure 5.8 represented the maximum hogging bending moment due to the seismic load in both x and z directions. The figure clearly indicated that for seismic load in both x and z direction (EQ X and EQ Z respectively), exterior longitudinal girder 1(exterior l. girder 1) had lesser value of hogging moment as compared to exterior longitudinal girder 2(exterior l. girder 2) all the models. Similarly, the interior longitudinal girder 3(interior l. girder 3) had highest value of hogging moment due to both EQ X and EQ Z for all the models. However, the value of hogging moment due to seismic load in x direction (EQ X) was greater than that of seismic load in z direction (EQ Z). In case of longitudinal girders, the maximum value of hogging moment was observed for model 5 (model with 60^o skew angle) for exterior longitudinal girder 2 under seismic load in x direction. Amongst the cross girders, the maximum hogging moment value was observed for exterior cross girders in all models under the seismic load in z and x direction respectively. The hogging moment in the cross girder increased with increase in skew angle. However, the value of hogging moment due to seismic load in z direction (EQ Z) was greater than that of seismic load in x direction (EQ X). In case of cross girders, the maximum value of hogging moment was observed for model 5 (model with 60° skew angle) for exterior cross girder 2 under seismic load in z direction.

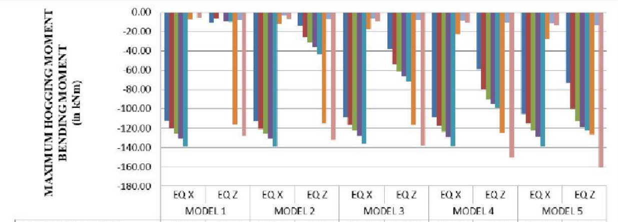

	MODEL 1 EQ X	MODEL 1 EQ Z	MODEL 2 EQ X	MODEL 2 EQ Z	MODEL 3 EQ X	MODEL 3 EQ Z	MODEL 4 EQ X	MODEL 4 EQ Z	MODEL 5 EQ X	MODEL 5 EQ Z
EXTERIOR-L.GIRDER 1	-112.26	-10.96	-112.93	-13.94	-108.30	-37.52	-108.44	-59.11	-104.99	-73.55
INTERIOR-L.GIRDER 1	-120.45	-6.62	-120.75	-25.97	-116.79	-53.78	-117.59	-79.92	-115.38	-99.81
INTERIOR-L.GIRDER 2	-125.65	-0.04	-125.77	-31.76	-122.33	-61.65	-123.57	-89.98	-122.25	-112.98
INTERIOR-L.GIRDER 3	-130.61	-9.69	-130.60	-36.10	-127.74	-66.32	-129.47	-94.71	-129.14	-118.73
EXTERIOR-L.GIRDER 2	-139.10	-10.39	-139.13	-43.40	-136.79	-72.48	-138.60	-99.13	-138.99	-122.47
EXTERIOR CROSS GIRDER 1	-7.45	-115.86	-12.32	-115.23	-17.90	-116.42	-22.40	-124.51	-27.46	-126.28
INTERIOR MID CROSS GIRDER	0.00	-8.15	-3.36	-7.16	-6.54	-7.91	-9.36	-10.99	-11.79	-13.35
EXTERIOR CROSS GIRDER 2	-5.39	-128.00	-7.16	-132.49	-9.49	-137.92	-10.94	-150.71	-13.37	-160.74

FIGURE 5.8: GRAPH SHOWING THE VARIATION OF MAXIMUM HOGGING MOMENT FOR VARIOUS MODELS UNDER SEISMIC LOAD IN BOTH X AND Z DIRECTION

B. Shear Force

Shear force also depends on the load applied on the structure. Various loads like dead load, live load (vehicular load), seismic load was applied on the bridge superstructure. For each of these load, the shear force developed on the longitudinal and cross girders of each model was noted and plotted and shown in figure 9 to 12.

B.1 Shear force due to dead load and footpath live load

Figure 5.9 represented the maximum shear force due to dead load and footpath live load. The figure clearly indicated that for all exterior girders (both longitudinal and cross girders) the maximum shear force increases with increase in skew angle but for all interior girders (both longitudinal and cross girders) the maximum shear force decreases with increase in skew angle. In case of longitudinal girders, the maximum value of shear force was observed for model 5 (model with 60° skew angle) for exterior longitudinal girder 2. Amongst the cross girders, the maximum value of shear force was observed for model 1 (model with 0° skew angle) for interior mid cross girder and the minimum value was observed for model 5(model with 60° skew angle) for interior mid cross girder.

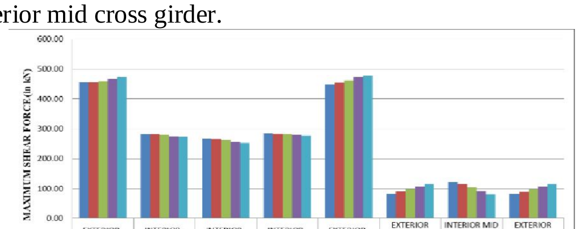

	EXTERIOR-L.GIRDER 1	INTERIOR-L.GIRDER 1	INTERIOR-L.GIRDER 2	INTERIOR-L.GIRDER 3	EXTERIOR-L.GIRDER 2	EXTERIOR CROSS GIRDER 1	INTERIOR MID CROSS GIRDER	EXTERIOR CROSS GIRDER 2
MODEL 1	454.85	282.23	268.87	284.39	448.11	81.60	121.33	81.60
MODEL 2	454.98	281.36	267.15	283.72	453.45	89.54	116.55	88.09
MODEL 3	459.49	278.89	262.61	281.58	462.17	99.09	104.86	97.83
MODEL 4	465.74	275.81	257.52	279.21	471.37	108.19	91.45	107.08
MODEL 5	471.30	273.12	253.53	277.35	478.69	115.11	80.50	114.27

FIGURE 5.9: GRAPH SHOWING THE VARIATION OF MAXIMUM SHEAR FORCE FOR VARIOUS MODELS UNDER DEAD LOAD AND FOOTPATH LIVE LOAD

B.2 Shear force due to live load

B.2.1 Live Load (Case 1 i.e., combination of Class 70 R (Wheeled) + Class A vehicles)

Figure 5.10 represented the maximum shear force due to live load (case 1 i.e., combination of class 70 R (wheeled) + class A vehicles). The figure clearly indicated that for all girders (both longitudinal and cross girders) except exterior cross girder 1 and 2, the maximum shear force increases with increase in skew angle upto 15° but then decreases. In exterior cross girder 1 and 2, the maximum shear force increased with increase in skew angle. In case of longitudinal girders, the maximum value of shear force was observed for model 1 (model with 0° skew angle) for interior longitudinal girder 3. Amongst the cross girders, the maximum value of shear force was observed for model 5 (model with 60° skew angle) for exterior cross girder 1 and the minimum value was observed for model 1 (model with 0° skew angle) for exterior cross girder 1.

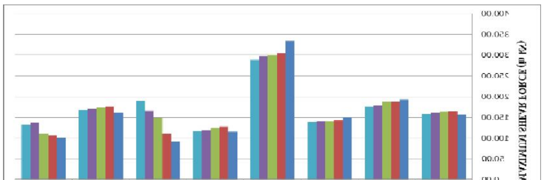

	EXTERIOR-L.GIRDER 1	INTERIOR-L.GIRDER 1	INTERIOR-L.GIRDER 2	INTERIOR-L.GIRDER 3	EXTERIOR-L.GIRDER 2	EXTERIOR CROSS GIRDER 1	INTERIOR MID CROSS GIRDER	EXTERIOR CROSS GIRDER 2
MODEL 1	157.64	192.36	151.33	334.08	114.82	92.56	161.41	102.28
MODEL 2	164.89	187.37	147.28	304.40	126.97	110.52	175.84	107.20
MODEL 3	163.79	187.66	139.93	300.77	123.58	149.35	172.83	109.21
MODEL 4	161.72	179.78	139.86	296.46	118.68	165.59	171.54	136.71
MODEL 5	158.25	176.33	138.48	288.21	116.32	189.56	167.78	131.73

FIGURE 5.10: GRAPH SHOWING THE VARIATION OF MAXIMUM SHEAR FORCE FOR VARIOUS MODELS UNDER LIVE LOAD (CASE 1 i.e., COMBINATION OF CLASS 70 R (WHEELED) + CLASS A VEHICLES)

B.2.2 Live Load (Case 2 i.e., combination of Class A + Class A + Class A vehicles)

Figure 5.11 represented the maximum shear force due to live load (case 2 i.e., combination of class A + class A + class A). The figure clearly indicated that in case of longitudinal girders, the maximum value of shear force was observed for model 1 (model with 0° skew angle) for interior longitudinal girder 2. Amongst the cross girders, the maximum value of shear force was observed for model 5 (model with 60° skew angle) for exterior cross girder 2 and the minimum value was observed for model 2 (model with 15° skew angle) for exterior cross girder 1.

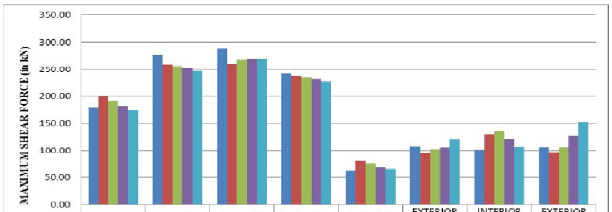

	EXTERIOR L.GIRDER 1	INTERIOR L.GIRDER 1	INTERIOR L.GIRDER 2	INTERIOR L.GIRDER 3	EXTERIOR L.GIRDER 2	EXTERIOR CROSS GIRDER 1	INTERIOR MID CROSS GIRDER	EXTERIOR CROSS GIRDER 2
MODEL 1	179.21	275.78	287.69	241.20	62.75	107.26	101.18	106.12
MODEL 2	199.35	258.73	259.49	236.80	80.85	93.96	128.91	96.37
MODEL 3	191.88	255.98	267.59	234.88	75.05	101.85	136.64	106.23
MODEL 4	181.37	252.19	268.91	230.99	69.32	105.44	120.69	127.07
MODEL 5	174.38	246.64	269.29	226.58	65.24	119.90	106.85	151.82

FIGURE 5.11: GRAPH SHOWING THE VARIATION OF MAXIMUM SHEAR FORCE FOR VARIOUS MODELS UNDER LIVE LOAD (CASE 2 i.e., COMBINATION OF CLASS A + CLASS A + CLASS A VEHICLES)

B.3 Shear force due to seismic load

Figure 5.12 represented the maximum shear force due to seismic load in both x and z direction (EQ X and EQ Z direction respectively). The figure clearly indicated that in case of longitudinal girders, the maximum value of shear force was observed for model 5 (model with 60^o skew angle) for exterior longitudinal girder 2 under the seismic loading in z direction and the minimum value was observed for model 1(model with 0^o skew angle) for interior longitudinal girder 1 under the seismic loading in x direction. Amongst the cross girders, the maximum value of shear force was observed for model 5 (model with 60^o skew angle) for exterior cross girder 2 under the seismic loading in x direction. However, the shear force on the cross girders was found to be very less compared to shear force on the longitudinal girders (especially exterior longitudinal girders).

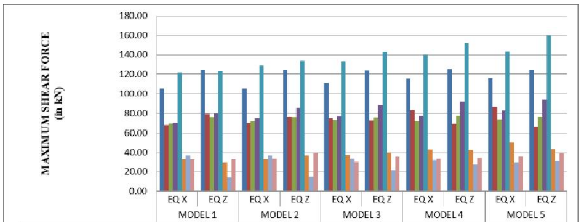

	MODEL 1 EQ X	MODEL 1 EQ Z	MODEL 2 EQ X	MODEL 2 EQ Z	MODEL 3 EQ X	MODEL 3 EQ Z	MODEL 4 EQ X	MODEL 4 EQ Z	MODEL 5 EQ X	MODEL 5 EQ Z
EXTERIOR-L.GIRDER 1	105.47	124.58	105.35	124.97	110.71	123.67	115.55	125.08	115.66	124.88
INTERIOR-L.GIRDER 1	67.79	79.69	70.61	76.25	74.56	72.62	83.59	68.99	86.73	65.87
INTERIOR-L.GIRDER 2	69.39	75.98	71.95	75.85	73.09	75.34	71.84	77.60	73.50	76.48
INTERIOR-L.GIRDER 3	70.32	80.14	74.52	85.22	76.92	88.57	77.72	92.07	82.81	93.98
EXTERIOR-L.GIRDER 2	121.23	122.72	128.53	133.68	133.39	142.52	139.66	152.42	143.18	160.06
EXTERIOR CROSS GIRDER 1	33.12	29.45	33.00	36.95	37.73	40.08	43.35	42.83	50.30	43.48
INTERIOR MID CROSS GIRDER	37.19	14.15	37.38	15.15	33.50	21.87	32.42	27.90	29.76	31.48
EXTERIOR CROSS GIRDER 2	33.18	33.11	33.71	40.19	30.15	35.62	33.51	34.70	35.94	39.29

FIGURE 5.12: GRAPH SHOWING THE VARIATION OF MAXIMUM SHEAR FORCE FOR VARIOUS MODELS UNDER SEISMIC LOAD IN BOTH X AND Z DIRECTION

VI. CONCLUSIONS

- From the above analysis results, the following conclusions were drawn.
- In general, it was observed that bending moment increased with increase in skew angle.
- Shear force variation did not follow any particular pattern to change with the change in skew angle.
- In case of dead load, the maximum hogging as well as sagging moment was observed on the exterior longitudinal girders.
- In case of live load (both case 1 and 2) , the interior longitudinal girders had the maximum sagging as well as hogging moments. However, amongst the cross girders, the exterior cross girder 2 had maximum sagging moment where as interior mid cross girder had maximum hogging moment.
- Similarly, in case of seismic load also the maximum bending moment was found on the exterior longitudinal girders (especially exterior longitudinal girder 2) as well as the exterior cross girders (especially exterior cross girder 2).
- The value of sagging moment as well as hogging moment due to seismic load in x direction (EQ X) was greater than that of seismic load in z direction (EQ Z) but the value of shear force due to seismic load in z direction (EQ Z) was greater than that of seismic load in x direction (EQ X) for all the 5 models.
- The shear force for exterior longitudinal girders and interior longitudinal girders increased and decreased with increase skew angle in case of dead load respectively but decreased in case of live loads. However, the pattern of shear force variation reversed in case of cross girders under these loads.
- In case of dead load as well as seismic load, the maximum shear force was observed on the exterior longitudinal girders where as in case of live loads, it was observed on the interior longitudinal girders. Under the seismic loads in both x and z direction , the shear force for longitudinal girders increased with increase in skew angle where as the pattern was random in case of cross girders.
- The seismic force would not affect the design of the bridge superstructure significantly since the value of maximum bending moment obtained due to it is very less as compared to other loads (almost 10 % of the maximum bending moment obtained due to dead load).From the analysis carried out and the conclusions drawn above it can be concluded that model 5 (model with 60o skew angle) had the maximum bending moment and shear force where as model 1 (model with 0o skew angle) had the

minimum bending moment and shear force amongst all five models.

REFERENCES

[1] Ahmed Abdel-Mohti and Gokhan Pekcan (2013), “Assessment of seismic performance of skew reinforced concrete box girder bridges”, International Journal of Advanced Structural Engineering, December 2013, 5:1

[2] Ansuman Kar, P.R. Maiti, Vikas khatri and P.K. Singh (2012), “study on effect of skew angle in skew bridges” International journal of Engineering Research and Department, ISSN: 2278-067X, P-ISSN: 2778-800X.

[3] Aref, A.J. et al. (2001), “Ritz-Based Static analysis Method for Fibre Reinforced Plastic Rib Core skew Bridge Superstructure”, Journal of Engineering Mechanics, 127(5), pp.450-458

[4] B.Bakhit (1988), “Analysis of some skew bridges as right Bridges”, Structural Engineering. Vol. 114(10).

[5] Bellman, R. (1973), “Methods of nonlinear analysis”, Academic Press, New York.

[6] Bishara, A. G., M. C. and El-A, Liu, li, N. D., “Wheel Load Distribution on Simply Supported Skew I-beam Composite Bridges.” Structural Engineering, ASCE, 119(2), (1993) pp.399-419.

[7] Ebeido (1996), “Shear and reaction distribution in skew composite bridges” Journal of bridge engineering, 1(4), pp.155-165

[8] Haung, H., Shenton, H.W. and Chajes, M.J. (2004), “Load distribution for highway skew bridges”, Journal of bridge Engineering, 9(6), pp.558-562

[9] Helba and Conradp Hiengs (1995), “Skew composite bridges-analysis for ultimate load”, Journal of Civil Engineering, 22(6), pp.1092-1103

[10] Himanshu Jaggerwal and Yogesh Bajpai (2014), “Effect of skewness on three span RC T-beam Bridges”, International Journal of Computational Engineering Research (IJCER) , ISSN (e): 2250 – 3005 || Vol, 04 || Issue, 8 || August – 2014

[11] IRC 6-2016,”Standard Specifications And Code Of Practice For Road Bridges Section: II Loads And Load Combinations (Seventh Revision)”

[12] K. Nguyena and J.M. Goicolea (2018), “Analytical and simplified models for dynamic analysis of short skew bridges under moving loads”, arXiv:1704.07285v2 [cs.CE] 12 Feb 2018

[13] Luke Chen and Suren Chen (2016), “Earthquake Fragility Assessment of Curved and Skewed Bridges in Mountain West Region”, MPC 16-312

[14] Mladen Ulićević , Nina Serdar, Srđan Janković (2015), “Influence of horizontal curvature radius and bent skew angle on seismic response of RC bridges”, DOI: https://doi.org/10.14256/JCE.1508.2015

[15] Nagashekhar J P, Dr.Mahadev M Achar, Dr.Ramesh Manoli, Shiva Kumar KS (2016), “Effect of skew on the behaviour of RC girder bridges”, International Research Journal of Engineering and Technology (IRJET) e-ISSN: 2395 -0056, p-ISSN: 2395-0072, Volume: 03 Issue: 07 | July-2016

[16] P. Pottatheere and P. Renault (2008), “Seismic vulnerability assessment of skew bridges”, The 14Th World Conference on Earthquake Engineering ,October 12-17, 2008, Beijing, China

[17] S.V. Joshi, Ajay D. Shahu, P. D. Pachpor(2016), “Analysis and behaviour of skew bridge with different skew angle”, ISSN (PRINT): 2393-8374, (ONLINE): 2394-0697, Volume-3, Issue-10, 2016.

[18] Shervin Maleki (2001), “Seismic design force for single-span slab-girder skewed bridges”, Electronic Journal of Structural Engineering, 2 (2001)

[19] Vaibhav Kothari and Pranesh Murnal (2015), “Seismic Analysis of Skew Bridges”, Journal of Civil Engineering and Environmental Technology ,Print ISSN: 2349-8404; Online ISSN: 2349-879X; Volume 2, Number 10; April-June, 2015 pp. 71-76